Earthq Eng & Eng Vib (2014) 13: 317-326 **DOI**: 10.1007/s11803-014-0233-1

Dynamic properties analysis of a stay cable-damper system in consideration of design and construction factors

Dan Danhui[1†], Chen Yanyang[2‡] and Xiao Rong[1§]

1. *Department of Bridge Engineering, Tongji University, Shanghai 200092, China*
2. *Henan Provincial Communications Planning Survey & Design Institute Co.,Ltd., Zhangzhou 450052, China*

Abstract: A numerical solution based on the Steffensen stable point iterative method is proposed to resolve the transcendental frequency equation of a stay cable-damper system. The frequency equation, which considers clamped supports and flexural rigidity of the cable, is intended to investigate the influence of the parameters of the cable damper system on its dynamic characteristics. Two factors involved in the design and construction phases, the damping coefficient induced by external dampers and the cable tension, are the focus of this study. Their impact on modal frequencies and damping ratios in these two phases of cable-damper systems are investigated by resolving the equation with the proposed solution. It is shown that the damping coefficient and cable tension exert more noticeable effects on the modal damping ratios than on the modal frequencies of stay cable-damper systems, and the two factors can serve as design variables in the design phase and as adjustment factors in the construction phase. On the basis of the results, a roadmap for system-level optimal design of stay cable-damper systems that can achieve global optimal vibration suppression for the entire bridge is proposed and discussed.

Keywords: cable; damper; damping coefficient; cable tension; dynamic property; optimal design

1 Background

Vibrations on long cables that become an increasingly serious problem as the spans of cable-stayed bridges expand. Excessive cable oscillation diminishes pedestrian perceptions of safety, reduces driver and passenger comfort, and causes fatigue coupled with corrosion and erosion in the strings of cable and anchorage zones. These defects decrease durability and endanger the overall safety of bridges. The most extensively applied vibration suppression measurement is the installation of external dampers at the end of stay cables to increase low-order modal damping ratios and reduce oscillation amplitude (Irvine, 1981). Damper installation changes the dynamic characteristics of cable-damper systems in three ways: modal shape, modal frequency, and modal damping. The extent and mechanism of influence of these factors are related to the parameters of the cable and the damper; those for the latter include damper category, damper coefficient, and manner of installation. Investigating the vibration suppression effect of external dampers necessitates exploring the dynamic properties of cable-damper systems.

The effects of dampers on the dynamic properties of stay cables are well documented. Using a numerical method, Pacheco *et al*. (1993) investigated the vibration of taut strings with intermediate dampers. Krenk re-studied this string-cable system by using an analytical method in 2000. The author extended his investigation with Krenk and Nielsen (2002) and Krenk (2004), considering the effects of sag on the dynamic properties of cables and accordingly modifying the aforementioned analytical method. Main and Jones (2002a, b) studied the dynamic properties of a taut string damper system under free vibration. A subsequent study by Main and Jones (2007a, b) covers the foundation of a cable-damper system, for which clamped end conditions were considered and a frequency characteristic equation was established. The dynamic properties of cable-damper systems, including fifth-order complex frequency and complex trace, as well as modal shape, have been studied under various installation positions of dampers. However, the vibration suppression effect is influenced

Correspondence to: Dan Danhui, Room 711, Bridge Building, Department of Bridge Engineering, Tongji University, 1239 Siping Road, Shanghai 200092, China
Tel: +86-21-67392819; Fax: +86-21-55042363
E-mail: dandanhui@tongji.edu.cn
[†]Associate professor; [‡]Engineer; [§]Master Candidate

Supported by: Key State Laboratories Freedom Research Project under Grant No. SLDRCE09-D-01; the Fundamental Research Funds for the Central Universities, the Project of National Key Technology R&D Program in the 12th Five Year Plan of China under Grant No. 2012BAJ11B01; National Natural Science Foundation of China under Grant No. 50978196; State Meteorological Administration Special Funds of Meteorological Industry Research under Grant No. 201306102; and the Ministry of Education of China under Grant No. 2008B090500222
Received February 5, 2013; **Accepted** September 27, 2013

not only by installation position, but also by other factors related to dampers and cables. Moreover, the target of vibration suppression is not limited to a few low-order modes. Under different design and construction conditions, the dynamic properties of stay cables after damper installation remain unclear and therefore require further study.

In this study, the cable tension is proven to have a marked influence on the systematic dynamic properties of a stay cable-damper system; it can be utilized in the design phase by selecting reasonable design cable tension to obtain an appropriate vibration suppression effect. Thus, in this study, both of the influences of the damping coefficient of laterally attached external dampers and cable tension on the systematic dynamic properties of a stay cable-damper system are examined. The investigation is based on the transcendental frequency equation formulated by Main and Jones (2007a, b), as well as on bending rigidity and clamped supports. A systematic technology roadmap of the design and construction of cable-damper systems is proposed. This roadmap makes it possible to transfer the target of vibration suppression to high-order modes and achieve an optimal suppression effect for the entire bridge system.

2 Numerical solution of the transcendental frequency equation of a cable-damper system consideing clamped supports and flexural rigidity

2.1 Frequency function for the cable-damper system

Consider the design and construction phases of an actual cable-damper system (see Fig. 1, where c is the damper coefficient, β is the nonlinear coefficient, k_d is the damper stiffness and k_s is the damper support stiffness). These phases are divided into three distinct steps: the tension, clamped, and damper installation. After the first step is completed, the mechanical model of the cable can be regarded as a taut cable with double-pinned boundary conditions. At this stage, bending rigidity is also considered. In the second step, both anchorage zones of the cable are clamped, after which the cable model can be considered subjected to rigid-jointed boundary conditions. In the third step, a cable-damper system is formed and can be modeled as a taut cable-damper system with double-clamped boundary conditions. In such a model, the inner damping of the cable is disregarded.

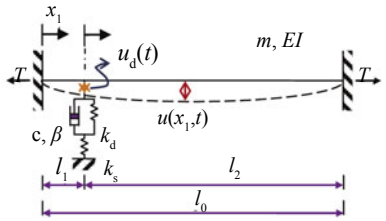

Fig. 1 Schematic of a stay cable-damper system

The oscillatory differential equation of a cable–damper system, in which the effect of cable sag is disregarded, can be written as follows:

$$EI\frac{\partial^4 u}{\partial x_j^4} - T\frac{\partial^2 u}{\partial x_j^2} + m\frac{\partial^2 u}{\partial t^2} = 0 \tag{1}$$

where x_j is the axial coordinate of the jth segment and j = 0, 1, 2, corresponding to the entire cable before installation. The short segment of a cable-girder joint points toward the damper location, where as the long segment points from the damper to the cable-pylon anchorage zone. u (x_j,t) is the transverse deflection in time t and coordinate. x_j is the cable tension, m denotes the mass per unit length, E is the Young's modulus, and I is the moment of cable inertia.

In reference to the cable-damper system shown in Fig. 1 and Eq. (1), Main and Jones (2002a, b) presented a transcendental frequency equation, in which the bending rigidity of the damper and its frame are disregarded . In the current work, a re-formulated expression of this frequency equation is provided for convenience:

$$Q_0^{\mathrm{CC}} + \mathrm{i}cl_0 \cdot \frac{\zeta}{\eta} \cdot \frac{p}{p^2+q^2} \cdot \left[Q_1^{\mathrm{CP}} Q_2^{\mathrm{CC}} + Q_1^{\mathrm{CC}} Q_2^{\mathrm{CP}} \right] = 0 \tag{2}$$

The frequency equation of a taut cable with a double-pinned boundary is

$$(1-\varepsilon_0{}^2)\sin(q) = 0 \tag{3}$$

The symbols in Eqs. (2) and (3) denote

$$Q_j^{\mathrm{CP}} = \left(1+\varepsilon_j^2\right)\sin(q\mu_j) - \frac{q}{p}\left(1-\varepsilon_j^2\right)\cos(q\mu_j) \tag{4}$$

$$Q_j^{\mathrm{CC}} = 2\varepsilon_j + \frac{\zeta T}{p^2}(1-\varepsilon_j^2)\sin(q\mu_j) - (1+\varepsilon_j^2)\cos(q\mu_j) \tag{5}$$

$$\varepsilon_j = \mathrm{e}^{-p\mu_j} \tag{6}$$

$$\left.\begin{matrix} p \\ q \end{matrix}\right\} = \sqrt{\sqrt{\zeta^2 T^2 + \eta^2\omega^2} \pm \zeta T} \tag{7}$$

In Eqs. (4)–(7), $\zeta = \dfrac{l_0^2}{2EI}$, $\eta = \sqrt{\dfrac{ml_0^4}{EI}}$, and l_0, l_1, l_2 are the length of each segment of the cable parameters of the cable-damper system, $l_0 = l_1 + l_2$, $\mu_j = l_j / l_0$. c is the damping coefficient of the damper. ω denotes the general complex frequency, with its real part reflecting the frequency of damped oscillation and its imaginary part reflecting the rate of decay.

Let $\theta = \{l_0, l_1, l_2, E, I, m, c, T\}$ denote the basic parameters of the cable-damper system. Equation (3) defines the implicit function of θ as

$$\omega_n^{\mathrm{PP}} = f(\theta) \tag{8}$$

When c = 0, Eq. (2) can be simplified into

$$2\mathrm{e}^{-p}+\frac{\zeta T}{p^2}(1-\mathrm{e}^{-2p})\sin q-(1+\mathrm{e}^{-2p})\cos q=0 \tag{9}$$

in which Eq. (9) defines the following implicit function:

$$\omega_n^{\mathrm{CC}}=h(\theta) \tag{10}$$

In the general situation $c \neq 0$, Eq. (2) defines the following implicit function:

$$\Omega_n^{\mathrm{CDC}}=g(\theta) \tag{11}$$

Given the existence of damping in Eqs. (8) and (11), Ω_n^{CDC} derived by Eq. (11) is generally complex. Modal frequencies and damping ratios can be easily derived using the following relationship:

$$\begin{cases}\omega_n^{\mathrm{CDC}}=\mathrm{real}(\Omega_n^{\mathrm{CDC}})\\ \xi_n^{\mathrm{CDC}}=\dfrac{\mathrm{imag}(\Omega_n^{\mathrm{CDC}})}{\mathrm{abs}(\Omega_n^{\mathrm{CDC}})}\end{cases} \tag{12}$$

When modeling the cable-damper system by taut string, the corresponding nth modal frequency can be given as follows

$$\omega_n^{\mathrm{s}}=\frac{n\pi}{l_0}\sqrt{\frac{T}{m}} \tag{13}$$

The influence ratio of the frequency induced by the different construction conditions of the cable-damper system can be defined as

$$\begin{cases}\Theta_n^{\mathrm{PP}\to\mathrm{CC}}=\dfrac{\omega_n^{\mathrm{CC}}-\omega_n^{\mathrm{PP}}}{\omega_n^{\mathrm{s}}}\\ \Theta_n^{\mathrm{CC}\to\mathrm{CDC}}=\dfrac{\omega_n^{\mathrm{CDC}}-\omega_n^{\mathrm{CC}}}{\omega_n^{\mathrm{s}}}\\ \Theta_n^{\mathrm{PP}\to\mathrm{CDC}}=\Theta_n^{\mathrm{CC}\to\mathrm{CDC}}+\Theta_n^{\mathrm{PP}\to\mathrm{CC}}=\dfrac{\omega_n^{\mathrm{CPC}}-\omega_n^{\mathrm{PP}}}{\omega_n^{\mathrm{s}}}\end{cases} \tag{14}$$

where $\Theta_n^{\mathrm{PP}\to\mathrm{CC}}$ is the influence ratio of the clamped boundary condition in Step 2. $\Theta_n^{\mathrm{CC}\to\mathrm{CDC}}$ represents the influence ratio of the damper in Step 3. $\Theta_n^{\mathrm{PP}\to\mathrm{CDC}}$ corresponds to the total influence ratio of the construction conditions; this ratio is equal to the sum of the first two influence ratios.

2.2 Numerical solution of the frequency equation, derived by the Steffensen fixed point iteration method

Despite the considerable difference in complexity of the implicit equations, their zero roots can be solved in a similar numerical manner; i.e., the secant or iteration method. Considering the most complicated implicit equations (Eqs. (2) and (11)), an iteration expression is presented to solve their zero roots in the complex field.

Substituting Eqs. (4)–(6) into Eq. (2) yields the simplified expression

$$\sin q\cdot A+\cos q\cdot B+C=0 \tag{15}$$

where

$$A=A_1+D\cdot[(1+\varepsilon_1^2\varepsilon_2^2)\frac{q^2-3p^2}{2p}-(\varepsilon_1^2+\varepsilon_2^2)\frac{p^2+q^2}{2p}+(1-\varepsilon_1^2\varepsilon_2^2)\frac{p^2+q^2}{q}\sin q\mu_1\cos q\mu_1+2p(\varepsilon_1+\varepsilon_1\varepsilon_2^2)\cos q\mu_1-2q(\varepsilon_1-\varepsilon_1\varepsilon_2^2)\sin q\mu_1] \tag{15a}$$

$$B=B_1+D\cdot[(1-\varepsilon_1^2\varepsilon_2^2)(q-\frac{p^2}{q}\sin^2 q\mu_1+q\cos^2 q\mu_1)-2p(\varepsilon_1+\varepsilon_1\varepsilon_2^2)\sin q\mu_1-2q(\varepsilon_1-\varepsilon_1\varepsilon_2^2)\cos q\mu_1] \tag{15b}$$

$$C=C_1+D\cdot[2p(\varepsilon_2+\varepsilon_1^2\varepsilon_2)\sin q\mu_1-2q(\varepsilon_2-\varepsilon_1^2\varepsilon_2)\cos q\mu_1] \tag{15c}$$

$$D=\mathrm{i}cl_0\cdot\frac{\zeta}{\eta}\cdot\frac{p}{p^2+q^2} \tag{15d}$$

and

$$A_1=\frac{\zeta T}{p^2}(1-\varepsilon_j^2),\quad B_1=-1-\varepsilon_0^2,\quad C_1=2\varepsilon_0$$

Considering the periodicity of the trigonometric function on the right side of Eq. (15), a transformed expression can be obtained:

$$q=f(q)=\begin{cases}n\pi-2\arctan\left(\dfrac{B+\dfrac{C-B}{2}\sec^2\dfrac{q}{2}}{A}\right) & n \text{ is even}\\ n\pi-2\,\mathrm{arccot}\left(\dfrac{2A+(C-B)\tan\dfrac{q}{2}}{C+B}\right) & n \text{ is odd}\end{cases} \tag{16}$$

On the basis of Eq. (16), the iteration expression derived by using the Steffensen fixed point method can be constructed as

$$\begin{cases}y_n=f(q_n),\quad z_n=f(q_n)\\ q_{n+1}=q_n-\dfrac{(y_n-q_n)^2}{z_n-2y_n+q_n}\end{cases} \tag{17}$$

From Eq. (7),

$$\omega=\sqrt{(q^4+2\zeta Tq^2)/\eta^2} \tag{18}$$

The iterations are repeated until q satisfies the requirements for accuracy. Then, q is substituted into Eq. (18) to obtain the solution of the numerical circular frequency of the cable-damper system.

3 Dynamic property analysis of the cable damper system

Under complicated real-world conditions, the

dynamic properties of cable-damper systems exhibit distinct discrepancies from those of taut string damper systems. These discrepancies occur in both low- and high-frequency ranges. Observation data (e.g., long-term records collected from the health monitoring systems installed in actual bridges) show that the vibration energies excited by natural vibration sources are more dominant at high rather than low-frequency modes; see Main and Jones (2002a, b). Extreme vibration cases also indicate that the first five lower frequency modes maintain low-level vibration energies that are drowned out by noise over the long term in bridge service. As wind speed increases, the dominant modes shift from a low-frequency to a considerably higher frequency range. Current passive cable damper system design theory is directed toward low-order modes, and the dampers installed in cables provide high damping ratios only for such modes, as reported by Weber *et al*. (2009a, b, c) and Weber and Boston (2011). Certain aspects of the vibration suppression effects induced by high-order modes and the dynamic properties of a cable-damper system at high frequencies are not well understood. This situation necessitates more comprehensive studies on these effects and properties.

In the design and construction phases of actual cable-stayed bridges, the design and selection of dampers are often a secondary priority. The upper connected points of dampers to cables are fixed to a certain height in order to be both aesthetically pleasing as well as practical. Although the damper position is a crucial parameter for adjusting the dynamic characteristics (Weber *et al*. 2007, 2009a, b, c), in practice, it can only be adjusted within a limited range. In these stages, only two factors — cable tension and damping coefficient — are valid adjustable parameters. Existing research focuses primarily on the influence of dampers on the dynamic characteristics of cables, with such influence determined on the basis of damper installation position, cable bending rigidity, and sag. For example, Boston *et al*. (2011) investigated numerically and experimentally optimal semi-active damping of a cable with flexural rigidity and clamped boundary conditions. In this study, a cable-damper system is considered as a whole and flexible rigidity and clamped boundary conditions are taken into account. The influence of the two adjustable factors (involved in the construction phase) on the modal frequencies and damping ratio of the cable-damper system are investigated by the numerical rooting method of the frequency equation presented in Eqs. (8), (10), and (11). The cable-damper system of a cable-stayed bridge in Shanghai's Changjiang Bridge is selected as an example. Its basic parameters are shown in Table 1.

For convenient comparison, an approximate damping ratio derived from an asymptotic damper design model that corresponds to ataut string damper system is presented (Krenk, 2000):

$$\xi_n^s \cong \frac{\pi^2 \kappa_n}{\left(\pi^2 \kappa_n\right)^2 + 1} \cdot \mu_1 \tag{19}$$

where κ_n is a commonly used dimensionless design parameter in linear damper design theory. This parameter is directly proportional to the damper coefficient and inversely proportional to the square root of the cable tension. It can be expressed as follows:

$$\kappa_n = \frac{c}{\pi\sqrt{Hm}} n\mu_1 \tag{20}$$

3.1 Influence of damper coefficient on the dynamic characteristic of cables

In general construction procedures, the damper is installed behind the cable. In this stage, the landscape of the entire bridge requires a fixed damper installation position. To obtain an optimal vibration suppression effect, therefore, the damping coefficient generated by the intermediate damper becomes the only effective optional adjustable factor. To investigate the influence of this factor on the dynamic properties of the cable-damper system, the damping coefficients listed in Table 1 are treated as variables, with scopes continuously varying from 10,000 N s/m to 10^6 N·s/m. Cable tension is set to 3×10^6 N, and the values indicated in Table 1 are retained for all other parameters. Each combination of parameters defines a scenario for the cable-damper system and yields a numerical frequency equation. Resolving the zero roots of the equations and repeatedly using the numerical methods proposed in Eqs. (12) , (14), and (19) yield the modal frequency, modal damping ratio, and influence ratio of frequency respectively.

The curve that reflects the relationship between the non-dimensional damper parameter and the influence ratios of the 1st to 11th frequency modes before and after the installation of dampers are illustrated in Fig. 2. Damper installation slightly increases the frequencies of all modes to 2%. The frequencies of all modes tend to increase as the damping coefficient rises. A tendency toward linear increases is observed at a κ of less than 0.3–0.4, but this tendency occurs at a gradual pace and then continuously increases when κ exceeds 0.3–0.4. In Fig. 2, the curves of odd and even modes are indicated

Table 1 Basic parameters of the stay cable-damper system

Length	Modulus	Moment of inertia	Density per length	Area	Inclined angle*	Damping coefficient of damper	Relative installation position of damper
97.6 m	2×10^{11} Pa	8.04×10^{-6} m^4	96.85 m	0.0124 m^2	0°	4×10^4 N·s/m	0.02

*Inclined angle refer to the angle between horizon direction and chord

in different colors: the dark red curves denote even anti-symmetric modes, whereas the blue curves denote odd symmetric modes. The increasing damping coefficient affects modal frequency in different ways. The damping coefficient imposes a stronger effect on even modes than on odd modes. At a constant damping coefficient, the influence ratio of even frequency modes gradually increases as order increases. By contrast, the influence ratio of odd frequency modes rapidly decreases as order increases.

The frequency influence ratios in different construction stages are compared in Fig. 3, where Figs. 3(a) and 3(b) correspond to damping coefficients of 10^5 and 5×10^5 N·s/m, respectively. Operation clamping enhances the frequency of each mode to about 1.6%. Damper installation also increases modal frequencies to different extents, and the increase in amplitude of higher order modes are greater than the lower order modes. Furthermore, the higher the damping coefficient produced by the damper, the higher the increase in all mode frequencies. In contrast to the same order in a taut string system, that the enhancement in frequency of the cable-damper system reaches 3.72%, which is a value that should be considered in analysis.

The influence of the damping coefficient on the modal damping ratios of the first 10 frequency modes is illustrated in Fig. 4, where the x axis represents a non-dimensional damper parameter and they axis represents the damping ratio (ξ_n) of the cable-damper system. The curve of the approximate damping ratio derived from the damper design and analytical model is also drawn in the same plot.

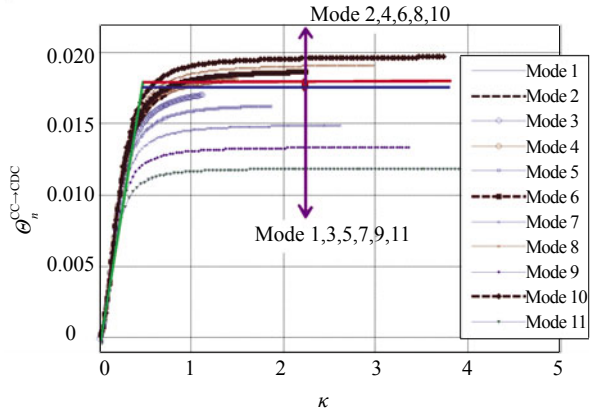

Fig. 2 Influence of the non-dimensional damper parameter on the first 11 frequency modes

Figure 4 shows an obvious difference between the damping ratios derived by the model of a taut string damper system with pinned boundary conditions and by the adaptive model of the cable-damper system with clamped boundary conditions. With regard to the taut string damper system, the curves corresponding to each mode coincide and peak at $\kappa_n^s \approx 1/\pi^2 = 0.1023$, where the optimum damping ratio of all modes ($\xi_n^s = 0.00998$) approaches half of the numerical relative damper installation position. When flexible rigidity and clamped boundary conditions are simultaneously considered in the mechanic model, the curves that correspond to each mode are scattered, with the highest degree of scatter occurring near the peaks of the curves. As the damping coefficient increases, all the modal damping ratios rapidly increase; after the ratios reach their peaks, they exhibit a mild decreasing tendency.

Further examination of the peak value of the 10th damping ratio indicates a remarkable discrepancy between the two models; i.e., in the asymptotic model, the peaks belonging to each mode overlap, but in the cable-damper system model, all the scattered peaks are lower than those of the asymptotic model, and the peaks move to the large side of the x axis. To extract the peak values from Fig. 4 and plot them against the mode orders shown in Fig. 5, the complicated behavior of peak values can be clarified by varying the discrepancy in the peak values of each mode in accordance with mode orders; that is, odd modes exhibit an increasing tendency, whereas even modes exhibit the opposite. If the peak value is defined as the optimal damping ratio and x ordinates (κ), where the peak value derived is the optimal non-dimensional damper parameter, it can be concluded that the optimal damping ratios derived by the asymptotic damper design model visibly loses precision.

The relative error of the optimal damping ratio is defined as

$$\delta_\xi = 100\times\left(\xi_n^{\mathrm{CDC}} - \xi_n^s\right)/\xi_n^s \tag{21}$$

The relative error of the optimal non-dimensional damper parameter is defined as

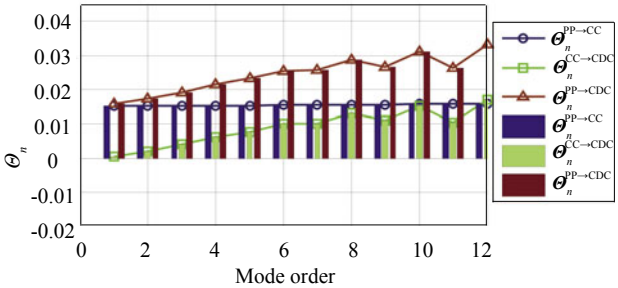

(a) $C = 10^5$ N·s/m

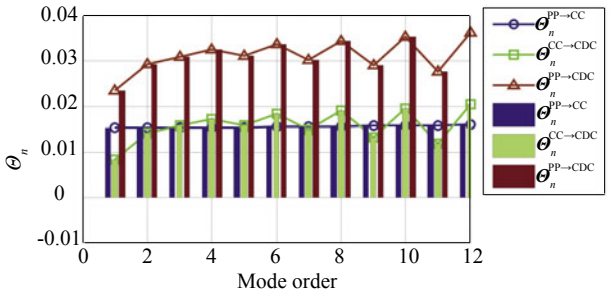

(b) $C = 5\times10^5$ N·s/m

Fig. 3 Comparison of the first 10 vibration modes before and after damper installation

$$\delta_{\mathrm{nd}} = 100 \times \left(\kappa_n^{\mathrm{CDC}} - \kappa_n^{\mathrm{s}} \right) / \kappa_n^{\mathrm{s}} \tag{22}$$

Table 2 presents a comparison of the optimal damping ratios and optimal non-dimensional damper parameters of the asymptotic and cable-damper system models. The optimal damping ratios of the first 10 frequency modes derived by the cable–damper system model are smaller than those obtained by the asymptotic damper design model. The largest discrepancy is 27.5%, obtained at the 7th mode, and the average discrepancy is 11.74%. The optimal non-dimensional damper parameters (of all the modes) obtained by the cable-damper system model are larger than those obtained by the asymptotic damper design model, with the largest discrepancy at 133.3% and the average discrepancy at 94.786%. These results indicate that using the asymptotic damper design model to choose and design dampers does not yield an optimal damping effect.

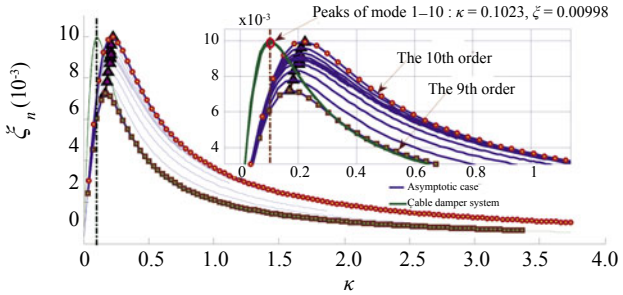

Fig. 4 Influence of the non-dimensional damper parameter on the first 10 modal damping ratios

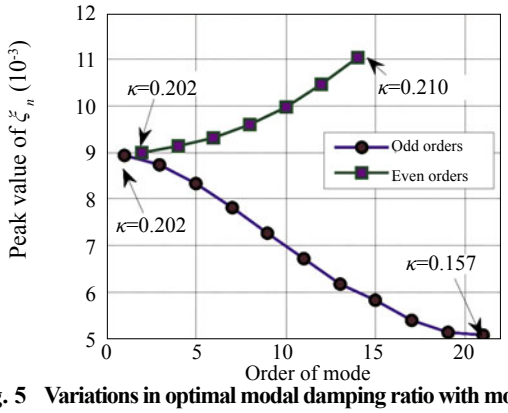

Fig. 5 Variations in optimal modal damping ratio with mode order

3.2 Influence of cable tension on the dynamic properties of cable-damper systems

As an integral force-bearing capacity system, cables have geometric and mechanical parameters that inevitably exert a direct influence on the dynamic properties of a system. Although factors such as cable sag, flexural rigidity, and clamped boundary conditions have been investigated and discussed in theoretical work, the general design procedures and concepts have not been fully considered. Damper parameters are optimally designed on the basis of these factors. In other words, fixed factors do not provide an adjustable function for identifying the optimal vibration damping effect. However, cable force can be adjusted to a relatively wider scope during construction. Cable tension can affect the final dynamic properties of a cable-damper system in the construction stage.

Let the cable tension vary at a scope of (3×10^5, 3×10^7 N), and the test parameters be fixed to a set of rational values in practice (Table 1). Note that the chosen variation range of the cable tension provides a possible scope for use in the design and construction stage. Once the design scheme is determined, it does not represent a realistic force variation range as it can occur due to live and dead loads and temperature. The frequency equations are numerically and repeatedly solved. The modal frequencies and damping ratios are calculated and their variation rules in relation to cable tension are investigated.

The influence curve of cable tension on the ultimate frequency influence ratio $\Theta_n^{\mathrm{CC}\to\mathrm{CDC}}$ that corresponds to odd and even modes are illustrated in Figs. 6(a) and 6(b). All the curves of the odd modes peak at about 2790 kN. Below this value, the frequency influence ratios rapidly increase from a negative value; beyond this peak, a slow decreasing tendency occurs. As cable tension increases, the frequencies of the even modes also increase and the peaks of the curves are not as obvious as those of the odd

Table 2 Comparison of the optimal modal damping ratios and non-dimensional damper parameters

Modes	Optimal damping ratio			Optimal non-dimensional damper parameter		
	ξ_n^{CDC}	ξ_n^{s}	δ_ξ (%)	κ_n^{CDC}	κ_n^{s}	δ_{nd} = (%)
1	0.0089	0.0100	–10.6	0.202	0.101	100
2	0.0090	0.0100	–9.92	0.202	0.105	92.86
3	0.0087	0.0100	–12.8	0.202	0.101	100
4	0.0091	0.0100	–8.74	0.209	0.105	100
5	0.0083	0.0100	–16.6	0.187	0.093	100
6	0.0093	0.0099	–6.34	0.202	0.112	80
7	0.0078	0.0100	–21.9	0.183	0.105	75
8	0.0096	0.0099	–3.2	0.209	0.09	133.3
9	0.0072	0.0100	–27.5	0.168	0.101	66.67
10	0.0100	0.0099	–0.227	0.224	0.112	100
Mean value	0.0088	0.00998	–11.74	0.1997	0.1023	94.786

modes. However, a somewhat decreasing trend in the ultimate frequency influence ratio is observed. Although the behaviors exhibited in this work are determined by a case study, a general conclusion can be drawn: cable tension distinctly affects modal frequency and the manner by which this influence is imposed differs depending on whether odd modes or even modes are considered.

The influence of cable tension on ultimate system damping ratios is also investigated. Figure 7(a) demonstrates the effect of cable force expressed with non-dimensional damper parameter κ on the damping ratio, where κ is inversely proportional to the square root of cable tension, and the blue curve corresponds to the curve of the asymptotic damper design model. When cable tension varies but other parameters are fixed, the variation rules of the final system damping ratio differ from those of the asymptotic damper design model. As cable tension increases, the peaks of the system damping ratio alternately occur at low to high vibration modes; under a high asymmetric mode, peaks do not occur and a continuous increasing trend takes place. Figure 7(b) illustrates the direct effect of cable force on the damping ratios of the cable-damper system. Similar conclusions can be drawn. The dotted box in the figure denotes the adjustment range of cable tension in the design and construction stages; the numerically adjusted cable tension is (1.5×10^6, 3.5×10^6), expressed in units of N. The damping ratios of each mode of the cable-damper system have a sufficient adjustment margin in this range, and the optimal damping ratios of important modes occur within this range.

The optimal damping ratios and the adjustable range of such ratios can be derived through the adjustment of cable force. The specific numerical results are provided in Table 3. Here, damping efficiency is defined as the percentage of the peak value of the damping ratio obtained by the cable-damper system model compared with that obtained by the asymptotic damper design model, i.e., $100\times\xi_n^{\mathrm{CDC}}/\xi_n^{\mathrm{s}}$ where $\xi_n^{\mathrm{s}}=0.0$ and is about half of the relative installation position of a damper. In engineering applications, adjusting cable tension within a feasible adjustment range markedly affects the final values of the systematic damping ratio. The extent of this effect differs from mode to mode. Among the modes investigated in this case study, the effects of the 5th, 7th, and 9th modes are the most dominant, with damping efficiencies of 54.6%, 66%, and 72.4%, respectively. The adjustable ranges of the damping ratio reach 0.00068, 0.00063, and 0.00149, respectively.

4 Design and construction factors for the systematic-level design of cable-damper systems

Three problems in the design of cable-damper systems are currently investigated (Weber, 2009a, b, c;

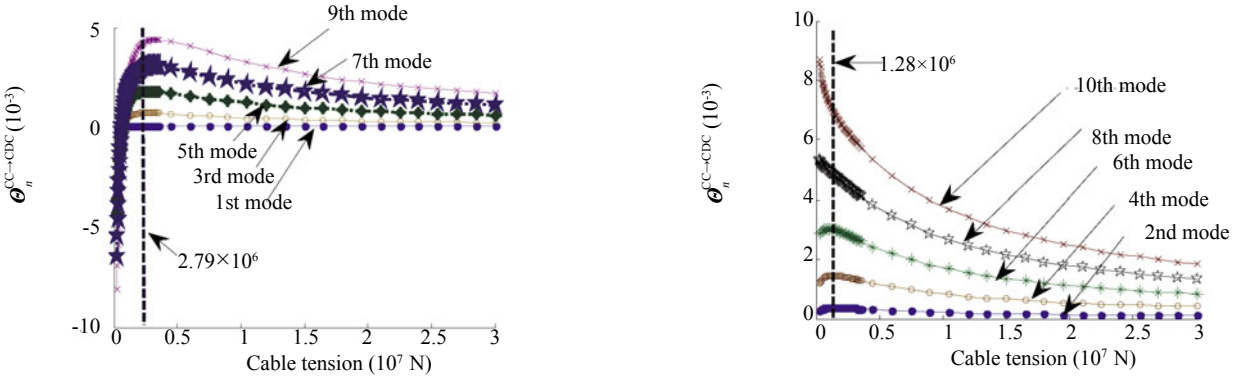

(a) Symmetric mode (b) Anti-symmetric mode

Fig. 6 Influence of cable tension on the change ratios of the first 10 frequency modes

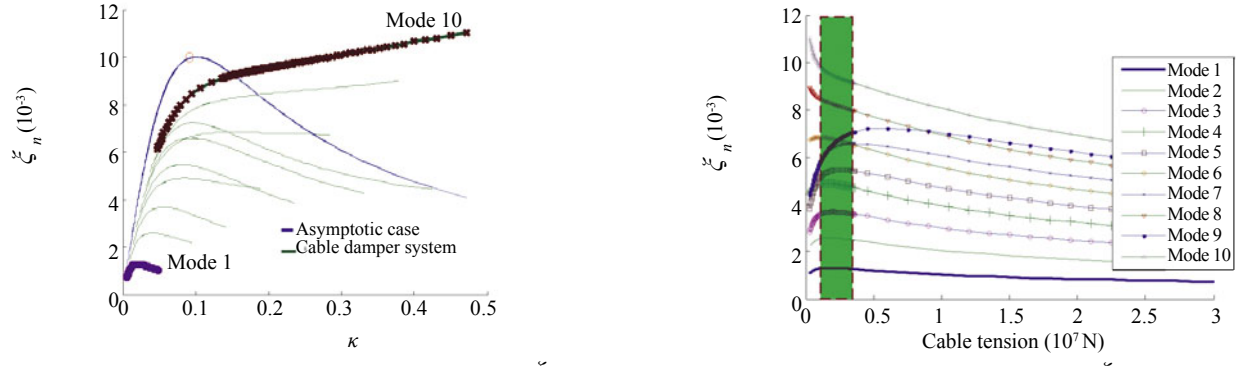

(a) Non-dimensional damper parameter vs. ζ (b) Cable tension vs. ζ

Fig. 7 Effect of cable tension on the damping ratios of the former10 modes of the cable-damper system

Huang and Jones, 2011; Fujino and Hoang, 2008). First, in practical engineering applications, the installation position of the dampers cannot be randomly chosen because of certain design constraints (for example, landscape demands). As a design variable, therefore, installation position cannot provide sufficient scope for adjustment and cannot facilitate the maximization of the damping effect in design. Second, in basic design methodologies, damper design is relegated to a secondary priority. Consequently, the range of design factors is restricted by cable parameters that are fixed in advance. The interaction between cables and dampers, as well as the optimal system-level design of dampers, is disregarded. Finally, as cable length increases, cable flexibility accordingly expands. As a result, vibration energy is distributed at high frequency ranges under ordinary excitation conditions. Current design methodologies do not consider high frequency modes and contradict the actual vibration behavior of cables. The working range of damper frequency should be tuned to higher modes, and the dynamic properties of the higher modes of cable-damper systems should be extensively investigated.

The discussion in the preceding sections indicates that the dynamic properties of cable-damper systems are influenced by both the parameters of dampers and cables. The ultimate damping effect pertains to the interaction of all the factors of a system. In designing dampers, according cables a position of equal importance to that of dampers, as well as achieving the optimal vibration suppression effect in bridges, is a worthwhile consideration. More specifically, the three levels of interactive design should be integrated. This integrationis formulated as follows.

Level one involves the design of an entire force-bearing cable system. After the basic design parameters are completed, maximizing the damping ratio of each cable attached with dampers should be set as one of the targets of optimal design. Adjusting cable tension in design and construction procedures enables the cable tension distribution in the cable group to match bridge configurations and rational distribution of inner force. This adjustment also enables the requirements for maximizing the vibration suppression of cable groups to be satisfied.

As illustrated in Fig. 8, determining the target damping ratio of a cable-damper system is incorporated into the adjustment of the cable system of an entire bridge. The adjustable damping ratio range can be determined by the adjustable range of cable tensions in the design and construction stages in accordance with the method proposed above. Then, the final target cable tension during bridge completion can be established on the basis of the maximum damping ratio range. Finally, automated cable tension adjustment enables the easy realization of the final target cable tension of each cable. Cable tension determined in this manner can be considered the synthesized optimal cable tension, which simultaneously takes vibration suppression, bridge configuration, and inner force distribution into account.

Level two involves the optimal design of a cable-damper system with the prerequisite basic cable design parameters and synthesized optimal cable tension. This level entails identifying a suitable installation position and selecting the optimal damper size or damping coefficient, with the aim of achieving the best vibration suppression effect. The case study shows that the final optimal damping ratios obtained by the cable-damper system deviates from that derived by the asymptotic damper design model; the optimal damping ratios at different modes also differ from one another. Accordingly, an individual design method for each cable is proposed on the basis of the numerical equation rooting method.

The third level revolves around determining the target vibration modes for a certain damper. The law of energy distribution on different vibration modes and frequencies should be analyzed and investigated on the basis of historical records and onsite data measurements, as well as on cable parameters and statistical data on the wind loads of local areas. For any typical cable, the mode whose vibration energy dominates throughout a year should be chosen as the candidate mode for vibration control. Other modes can also be considered to attain multi-mode vibration control. In doing so, the statistical law of energy distribution of the different modes in typical cables should be determined from the historical data collected from the acceleration sensors installed on cables. This law can serve as a design reference for new cable-damper systems located in the same area.

Table 3 Influence of tunable cable tension on the first 10 orders of optimal modal damping ratios

Mode	Optimal damping ratio	Optimal cable tension ($\times 10^6$ N)	Damping efficiency (%)	Adjustable range of damping ratio
1	0.00131	1.83	13.1	[0.00130, 0.00142]
2	0.00259	1.71	25.9	[0.00232, 0.00259]
3	0.00369	2.07	36.9	[0.00333, 0.00369]
4	0.00490	1.53	49.0	[0.00431, 0.00490]
5	0.00546	2.58	54.6	[0.00478, 0.00549]
6	/*	/	/	[0.00610, 0.00667]
7	0.00659	3.6	66.0	[0.00580, 0.00643]
8	/*	/	/	[0.00812, 0.00847]
9	0.00723	6.01	72.4	[0.00583, 0.00732]
10	/*	/	/	[0.00912, 0.00965]

* The peaks of modes 6th, 8th, and 10th are beyond the adjustable range of cable tension.

The numerical rooting method for determining the frequency equation of a cable-damper system is easily implementable by software or simplified computing programs. Therefore, individual design of cable-damper systems under general engineering conditions that are intended to achieve the best vibration control effect is feasible. The proposed method can compensate for the drawbacks of current damper design methods.

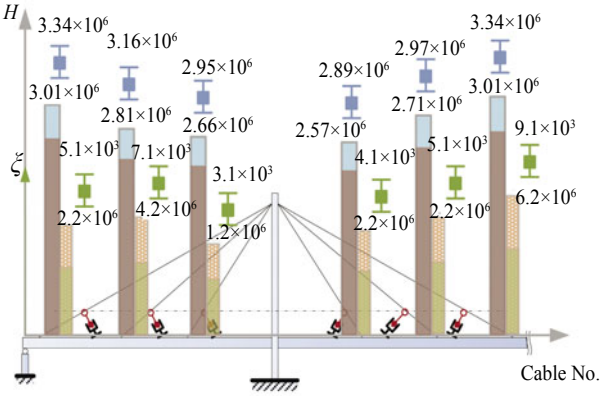

Fig.8 Schematic of the tension adjustment of the cable system for the maximization of vibration suppression

5 Conclusions

A numerical method is used to determine the root of the frequency equation of a cable-damper system; from this equation, the dynamic properties of the system can be derived. Two factors related to the design and construction stages of cable-damper systems are investigated to explore the mechanism of influence of such factors on the dynamic properties of the system. The conclusions drawn are summarized as follows.

(1) The influence of the damping coefficient and cable tension on modal frequencies does not exceed 2%, a value that accurately matches the influence exerted by clamped boundary conditions and flexible stiffness. The mechanisms of influence of the aforementioned parameters differ between odd and even modes.

(2) Damping coefficient and cable tension visibly influence the modal damping ratio of the cable-damper system. Consequently, these two factors can be chosen as design parameters. The adjustment of the cable tension can significantly improve the modal damping ratios of certain modes.

(3) The asymptotic damper design model (which considers a taut string damper system) differs from the cable-damper system in terms of the final modal damping ratio of the system, confirming that the latter is a more reasonable tool for designing cable-damper systems. The difficulty presented by the proposed numerical rooting method will not prevent the application of the cable-damper system model in engineering.

The conclusions support the proposed systematic-level damper optimal design methodology from the perspective of the holistic design of bridge cable systems; that is, individual design methodologies should be considered to realize the best vibration suppression effect on cable groups in entire bridges. Three other aspects should be taken into account: the adjustment of cable tension, the selection of optimal damper size guided by the numerical equation rooting method, and the rational selection of vibration modes for suppression guided by the statistical law determined from historical data on cables in similar conditions.

Acknowledgement

This research was sponsored by the Natural Science Fund Project (50978196), the Autonomous Project of State Key Laboratory (SLDRCE09-D-01), and the Combined Project of Production, Study and Research of the Provincial Department of the Ministry of Education of Guangdong Province (2008B090500222).

References

Boston C, Weber F and Guzzella L (2011), "Optimal Semi-active Damping of Cables with Bending Stiffness," *Smart Materials and Structures*, **20**(5): 8–15.

Fujino Y and Hoang N (2008), "Design Formulas for Damping of a Stay Cable with a Damper,"*Journal of Structural Engineering*, ASCE, **134**(2): 269–278.

Huang ZH and Jones NP (2011), "Damping of Taut-Cable Systems: Effects of Linear Elastic Spring Support," *Journal of Engineering Mechanics*, ASCE, **137**(7): 512–518.

Irvine HM (1981), *Cable Structures*, The MIT Press, Cambridge, Massachusetts, USA.

Krenk S (2000), "Vibrations of a Taut Cable with an External Damper," *Journal of Applied Mechanics*, **67**(4): 772–776.

Krenk S (2004), "Complex Modes and Frequencies in Damped Structural Vibrations,"*Journal of Sound and Vibration*, **270**(4–5): 981–996.

Krenk S and Nielsen SRK (2002), "Vibrations of a Shallow Cable with a Viscous Damper," *Proceedings of Royal Society A: Mathematical, Physical and Engineering Sciences*, London, **458**(2018): 339–357.

Main JA (2002), "Modeling the Vibrations of a Stay Cable with Attached Damper," *PhD Dissertation*, The Johns Hopkins University, pp.31–32.

Main JA and Jones NP (2002a), "Free Vibrations of a Taut Cable with Attached Damper. I: Linear Viscous Damper," *Journal of Engineering Mechan*ics, ASCE, **128**(10): 1062–1071.

Main JA and Jones NP (2002b), "Free Vibrations of a Taut Cable with Attached Damper. II: Nonlinear Damper," *Journal of Engineering Mechanics*, ASCE, **128**(10): 1072–1081.

Main JA and Jones NP (2007a), "Vibration of Tensioned Beams with Intermediate Damper. I: Formulation, Influence of Damper Location,"*Journal of Engineering Mechanics,* ASCE, **133**(4): 369–378.

Main JA and Jones NP (2007b), "Vibration of Tensioned Beams with Intermediate Damper. II: Damper near a Support," *Journal of Engineering Mechanics*, ASCE, **133**(4): 379–388.

Pacheco BM, Fujino Y and Sulekh A (1993), "Estimation Curve for Modal Damping in Stay Cables with Viscous Damper," *Journal of Structural Engineering*, **119**(6): 1961–1979.

Weber F and Boston C (2011), "Clipped Viscous Damping with Negative Stiffness for Semi-active Cable Damping," *Smart Materials and Structures*, **20**(4): 13–19.

Weber F, Boston C,Feltrin G and Motavalli M (2009a), "Cable Damping with Friction and Combined Viscous-Friction Dampers," *IV ECCOMAS, Thematic Conference on Smart Structures and Materials*, on CD, pp.345–352.

Weber F, Dist H, Feltrin G and Motavalli M (2009b), "Cycle Energy Control of MR Dampers on Cables," *Smart Materials and Structures*, **18**(1): 16–21.

Weber F, Distl H, Huber P, Nützel O and Motavalli M (2007), "Design, Implementation and Field Test of the Adaptive Damping System of the Franjo Tudjman Bridge nearby Dubrovnik, Croatia," *Proceedings of the IABSE Conferenc*e *2007*, Weimar, on CD, pp.39–46.

Weber F, Feltrin G, Maślanka M, Foboc W and Distl H (2009c), "Design of Viscous Dampers Targeting Multiple Cable Modes," *Engineering Structures*, **31**(11): 2797–2800.